

https://doi.org/10.1093/pnasnexus/pgad417 Advance access publication 14 December 2023 Research Report

# A statistical mechanics framework for constructing nonequilibrium thermodynamic models

Travis Leadbetter  $\mathbb{D}^a$ , Prashant K. Purohit  $\mathbb{D}^b$  and Celia Reina  $\mathbb{D}^{b,*}$ 

<sup>a</sup>Graduate Group in Applied Mathematics and Computational Science, University of Pennsylvania, Philadelphia, PA 19104, USA <sup>b</sup>Department of Mechanical Engineering and Applied Mechanics, University of Pennsylvania, Philadelphia, PA 19104, USA \*To whom correspondence should be addressed: Email: creina@seas.upenn.edu

Edited By: Pradeep Sharma

#### **Abstract**

Far-from-equilibrium phenomena are critical to all natural and engineered systems, and essential to biological processes responsible for life. For over a century and a half, since Carnot, Clausius, Maxwell, Boltzmann, and Gibbs, among many others, laid the foundation for our understanding of equilibrium processes, scientists and engineers have dreamed of an analogous treatment of nonequilibrium systems. But despite tremendous efforts, a universal theory of nonequilibrium behavior akin to equilibrium statistical mechanics and thermodynamics has evaded description. Several methodologies have proved their ability to accurately describe complex nonequilibrium systems at the macroscopic scale, but their accuracy and predictive capacity is predicated on either phenomenological kinetic equations fit to microscopic data or on running concurrent simulations at the particle level. Instead, we provide a novel framework for deriving standalone macroscopic thermodynamic models directly from microscopic physics without fitting in overdamped Langevin systems. The only necessary ingredient is a functional form for a parameterized, approximate density of states, in analogy to the assumption of a uniform density of states in the equilibrium microcanonical ensemble. We highlight this framework's effectiveness by deriving analytical approximations for evolving mechanical and thermodynamic quantities in a model of coiled-coil proteins and double-stranded DNA, thus producing, to the authors' knowledge, the first derivation of the governing equations for a phase propagating system under general loading conditions without appeal to phenomenology. The generality of our treatment allows for application to any system described by Langevin dynamics with arbitrary interaction energies and external driving, including colloidal macromolecules, hydrogels, and biopolymers.

Keywords: thermodynamics with internal variables, stochastic thermodynamics, variational approximation

#### Significance Statement

The beautiful connection between statistical mechanics and equilibrium thermodynamics is one of the crowning achievements in modern physics. Significant efforts have extended this connection into the nonequilibrium regime. Impactful, and in some cases surprising, progress has been achieved at both the macroscopic and microscopic scales, but a key challenge of bridging these scales remains. In this work, we provide a framework for constructing macroscopic nonequilibrium thermodynamic models from microscopic physics without relying on phenomenology, fitting to data, or concurrent particle simulations. We demonstrate this methodology on a model of coiled-coil proteins and double-stranded DNA, producing the first analytical approximations to the governing equations for a phase transforming system without phenomenological assumptions.

#### Introduction

Understanding and predicting far-from-equilibrium behavior is of critical importance for advancing a wide range of research and technological areas including dynamic behavior of materials, (1, 2), complex energy systems (3), as well as geological and living matter (4, 5). Although our understanding of each of these diverse fields continues to grow, a universal theory of nonequilibrium processes has remained elusive. The past century, however, has seen numerous significant breakthroughs toward this ultimate goal, of which we detail only a few below. At the macroscopic

scale, classical irreversible thermodynamics leverages the local equilibrium assumption to allow classical thermodynamic quantities to vary over space and time, enabling one to describe well-known linear transport equations such as Fourier's and Fick's laws (6). Extended irreversible thermodynamics further promotes the fluxes of these quantities to the level of independent variables in order to capture more general transport laws (7). Further extensions to allow for arbitrary state variables (not just fluxes), or history dependence take the names of thermodynamics with internal variables (TIV) or rational thermodynamics, respectively (8–11). More recently, the General Equation for Nonequilibrium Reversible-



Competing Interest: The authors declare no competing interest. Received: October 17, 2023. Accepted: November 22, 2023

© The Author(s) 2023. Published by Oxford University Press on behalf of National Academy of Sciences. This is an Open Access article distributed under the terms of the Creative Commons Attribution-NonCommercial-NoDerivs licence (https://creativecommons.org/licenses/by-nc-nd/4.0/), which permits non-commercial reproduction and distribution of the work, in any medium, provided the original work is not altered or transformed in any way, and that the work is properly cited. For commercial re-use, please contact journals.permissions@oup.com

Irreversible Coupling (GENERIC) framework and Onsager's variational formalism have proven to be successful enhancements of the more classical methods (12–15). On the other hand, linear response theory and fluctuation-dissipation relations constitute the first step toward a theory of statistical physics away from equilibrium. In the last few decades, interest in microscopic far-fromequilibrium processes has flourished due to the unforeseen discovery of the Jarzynski equality and other fluctuation theorems, as well as the advent of stochastic thermodynamics (16–20), and the application of large deviation theory to statistical physics (21–23). These advances have changed the way scientists view thermodynamics, entropy, and the second law particularly at small scales.

More specific to this work is the challenge of uniting scales. Given the success of the aforementioned macroscopic thermodynamic theories, how can one derive and inform the models within them using microscopic physics? Describing this connection constitutes the key challenge in formulating a unified far-from-equilibrium theory. As of yet, the GENERIC framework possesses the strongest microscopic foundation. Starting from a Hamiltonian system, one can either coarse grain using the projection operator formalism (24) or a statistical lack-of-fit optimization method (25, 26) in order to derive the GENERIC equations. However, these methods are either challenging to implement, analytically or numerically, or contain fitting parameters which must be approximated from data. Alternatively, one can begin from a special class of stochastic Markov processes and use fluctuation-dissipation relations or large deviation theory to the same effect (27, 28). So far, numerical implementations of these methods have only been formulated for purely dissipative systems, with no reversible component.

For this work, we shall utilize the less stringent framework of TIV, but recover GENERIC in an important case utilized in the examples. We will show how to leverage a variational method proposed by Eyink (29) for evolving approximate nonequilibrium probability distributions to derive the governing equations of TIV for systems whose microscopic physics is well described by Langevin dynamics. Furthermore, in the approach proposed here, the variational parameters of the probability density are interpreted as macroscopic internal variables, with dynamical equations fully determined through the variational method. Once the approximate density is inserted into the stochastic thermodynamics framework, the equations for the classical macroscopic thermodynamics quantities including work rate, heat rate, and entropy production appear naturally, and possess the TIV structure. For example, the internal variables do not explicitly appear in the equation for the work rate, and the entropy production factors into a product of fluxes and their conjugate affinities, which themselves are given by the gradient of a nonequilibrium free energy. Moreover, we show that when the approximating density is assumed to be Gaussian, the internal variables obey a gradient flow dynamics with respect to the nonequilibrium free energy, and so the resulting rate of entropy production is guaranteed to be nonnegative. This direct link between microscopic physics and TIV has not been elaborated elsewhere, and we refer to this method as stochastic thermodynamics with internal vari-

To illustrate and highlight the effectiveness of this method, we provide the results of two examples. The first is a paradigmatic example from stochastic thermodynamics: a single colloidal particle acted on by a linear external force, mimicking a macromolecule in an optical trap. It demonstrates all of the key features of the method while being simple enough to allow for comparison to exact solutions. The second example features a model system for studying

phase transitions of biomolecules, for example, in coiled-coil proteins (30, 31) (depicted in Fig. 1) or double-stranded DNA (32, 33): a colloidal mass–spring–chain system with double-well interactions between neighboring masses. By comparing to Langevin simulations, we show that STIV not only produces accurate analytical approximations to relevant thermodynamic quantities but also predicts the speed of a traveling phase front induced by external driving.

# Theory

#### Stochastic thermodynamics

We begin by outlining the key ideas of stochastic thermodynamics which defines classical thermodynamic quantities at the trajectory level for systems obeying Langevin dynamics, such as those embedded in an aqueous solution. These quantities include work, heat flow, and entropy production among others, and these new definitions allow for an expanded study of far-from-equilibrium behavior at the level of individual, fluctuating trajectories. Stochastic thermodynamics is a highly active area of study, and has been developed far beyond what is detailed here, as we have limited our presentation to only what we need for introducing STIV. We primarily follow the presentation of Seifert (19) throughout. Further details can be found in that work and in the references therein.

The paradigmatic example within stochastic thermodynamics is a colloidal particle in a viscous fluid at constant temperature, T, acted on by an external driving protocol (we present the theory for a single particle in one dimension, as the generalization to many particles in multiple dimensions is straightforward). This system is well described by an overdamped Langevin equation, which can be written as a stochastic differential equation of the form

$$dx(t) = -\frac{1}{\eta} \frac{\partial e}{\partial x}(x, \lambda) dt + \sqrt{2d} db(t),$$

where x(t) denotes the particle's position at time  $t \in [t_i, t_f]$ ,  $\eta$  is the drag coefficient of the particle in the fluid,  $-\frac{\partial e}{\partial x}(x,\lambda)$  is the force acting on the particle coming from a potential energy,  $e,\lambda(t)$  is a prescribed external control protocol,  $d=\frac{1}{\eta\beta}$  is the diffusion coefficient,  $\beta=1/k_BT$  is the inverse absolute temperature in energy units, and b(t) is a standard Brownian motion. We note that one may also include nonconservative interactions and external forces to model active noise within stochastic thermodynamics, but we do not use this feature in the current framework.

Given this system, stochastic thermodynamics enables one to define the internal energy, work, heat, and entropy at the level of the trajectory. Naturally,  $e(x(t), \lambda(t))$  defines the internal energy of the system. One does work on the system by changing e via the external control,  $\lambda$ . Thus, the incremental work reads

$$dw = \frac{\partial e}{\partial \lambda} \dot{\lambda} dt. \tag{1}$$

Using the first law of thermodynamics, we conclude that the incremental heat flowing out of the system is

$$dq = dw - de$$
.

An additional important quantity is the total entropy,  $s^{tot}$ . From the second law of thermodynamics, its macroscopic counterpart,  $S^{tot}$  (to be defined), should be nondecreasing and describes the level of irreversibility of the trajectory. To that end, the change in total entropy is defined using the log of the (Raydon–Nikodym) derivative of the probability of observing the given trajectory,  $\mathbb{P}[x(t) \mid \lambda]$ ,

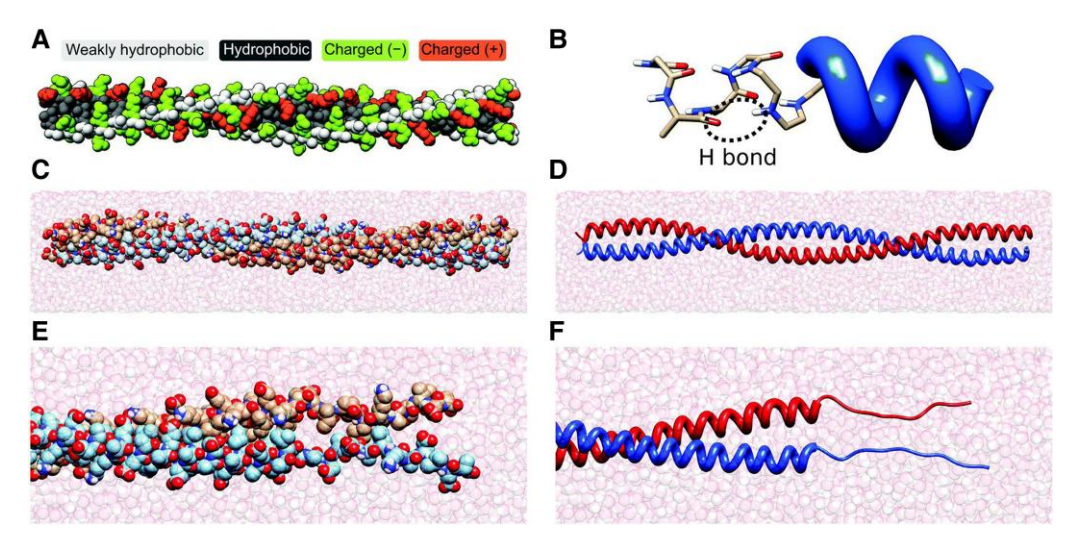


Fig. 1. The stochastic thermodynamics with internal variables (STIV) framework proposed here provides kinetic and thermodynamic equations for a broad class of systems described by Langevin dynamics, including the coiled-coil protein depicted in these snapshots. Taken from molecular dynamics simulations, atomic level structures are depicted in C) and E), while the unfolding due to an externally applied load becomes clear in the secondary structures shown in D) and F). The reference atomic structure and secondary structures are shown in A) and B). Vital for the coiled-coil protein's function, we study the dynamics of this transition from folded to unfolded configuration as a demonstration of the power of the STIV framework. Reproduced from Torres-Sánchez et al. (31) with permission from the Royal Society of Chemistry.

with respect to the probability of observing the reversed trajectory under the time reversed external protocol,  $\tilde{\mathbb{P}}[\tilde{x}(t) \mid \tilde{\lambda}]$ 

$$\Delta s^{tot}[x(t)] = k_B log \Biggl( \frac{d\mathbb{P}[x(t)\mid\lambda]}{d\tilde{\mathbb{P}}[\tilde{x}(t)\mid\tilde{\lambda}]} \Biggr),$$

where  $\tilde{x}(t) = x(t_f - t)$  and likewise for  $\tilde{\lambda}$  (34). Upon taking the expectation with respect to all possible trajectories (and any probabilistic initial conditions),

$$\Delta S^{\text{tot}} = \langle \Delta s^{\text{tot}} \rangle_{\text{paths}} = \int \!\! \Delta s^{\text{tot}}[x(t)] \, \mathrm{d}\mathbb{P}[x(t) \mid \lambda]$$

is recognized as  $k_B$  times the Kullback-Leibler divergence between the distributions of forward and backwards trajectories. As such,  $\Delta S^{tot}$  must be nonnegative. It is also useful to break up the total entropy change into the change in the entropy of the system (19),

$$\Delta s[x(t)] = -k_B \log \left( \frac{p(x(t_f), t_f \mid \lambda)}{p(x(t_i), t_i \mid \lambda)} \right),$$

where  $p(x, t | \lambda)$  is the probability density of observing the particle at position x at time t, and the change in the entropy of the medium

$$\Delta s^{m} = \Delta s tot - \Delta s. \tag{2}$$

Finally, one defines the microscopic nonequilibrium free energy in terms of the potential and entropy as  $a^{\text{neq}} = e - \text{Ts}$  (35). Using the path integral representation of  $\mathbb{P}[x(t) \mid \lambda]$  and  $\mathbb{\tilde{P}}[\tilde{x}(t) \mid \tilde{\lambda}]$ , one finds that the incremental heat dissipated into the medium equals the incremental entropy change in the medium  $Tds^m = dq$  (36). This allows one to relate the change in nonequilibrium free energy to the work done and the change in total entropy

$$da^{\text{neq}} = de - Tds$$

$$= dw - dq - Tds$$

$$= dw - Tds^{\text{tot}}.$$
(3)

As we saw with  $\Delta S^{tot}$ , each microscopic quantity has a macroscopic counterpart defined by taking the expectation with respect to all possible paths. Throughout, we use the convention that macroscopic (averaged) quantities are written in capital, and microscopic quantities are written in lower case, e.g.  $A^{\text{neq}} = \langle a^{\text{neq}} \rangle_{\text{naths}}$ .

#### Thermodynamics with internal variables

Now we turn to the macroscopic description, and give a brief overview of TIV. TIV has enjoyed decades of application as an important tool of study for irreversible processes in solids, fluids, granular media, and viscoelastic materials (37-41). Originally formulated as an extension to the theory of irreversible processes, TIV posits that nonequilibrium description without history dependence requires further state variables beyond the classical temperature, number of particles, and applied strain (in the canonical ensemble, for example) in order to determine the system's evolution (8, 42). These additional variables, the internal variables, encode the effects of the microscopic degrees of freedom on the observable macrostate. Thus, the relevant state functions take both classical and internal variables as input. The flexibility of the theory is apparent from the wide range of material behavior it can describe. The challenge, however, is in selecting descriptive internal variables, and in defining their kinetic equations in a way which is consistent with microscopic physics. Here, we take on the latter challenge.

#### Variational method of Eyink

The key mathematical tool we utilize for connecting TIV to stochastic thermodynamics is a variational method for approximating nonequilibrium systems laid out by Eyink (29). This method generalizes the Rayleigh-Ritz variational method of quantum mechanics to non-Hermitian operators. The method assumes the system in question can be described by a probability density function governed by an equation of the form  $\frac{\partial}{\partial t}p = \mathcal{L}p$ (e.g. a Fokker-Planck equation associated with Langevin particle dynamics). Since the operator  $\mathcal{L}$  is not Hermitian,  $\mathcal{L} \neq \mathcal{L}^{\dagger}$ , one must define a variational method over both probability densities p and test functions  $\psi$ . Begin by defining the nonequilibrium action functional

$$\Gamma[\psi, p] = \int_0^\infty \int_X \psi \left(\frac{\partial}{\partial t} - \mathcal{L}\right) p dx dt.$$

Under the constraint that

$$\int_{X} \psi p dx \Big|_{t=\infty} = \int_{X} \psi p dx \Big|_{t=0}$$

this action is stationary,  $\delta\Gamma[\psi^*,p^*]=0$ , if and only if  $(\frac{\partial}{\partial t}-\mathcal{L})p^*=0$  and  $(\frac{\partial}{\partial t}+\mathcal{L}^\dagger)\psi^*=0$ . By defining the nonequilibrium "Hamiltonian"  $\mathcal{H}[\psi,p]=\int_X\psi\;\mathcal{L}p\;\mathrm{d}x$ , one can recast the variational equation  $\delta\Gamma[\psi^*,p^*]=0$  in Hamiltonian form

$$\frac{\partial}{\partial t} p^* = \frac{\delta}{\delta u} \mathcal{H}[\psi^*, p^*] \tag{4}$$

$$\frac{\partial}{\partial t}\psi^* = -\frac{\delta}{\delta p}\mathcal{H}[\psi^*, p^*]. \tag{5}$$

As it stands, the variation is taken over two infinite dimensional function spaces, and as such, it is only possible to find exact solutions for a handful of systems. However, one can still make use of these dynamical equations to find a variational approximation to the true solution which lies within some fixed subspace. To do so, one begins by assuming the true density,  $p^*(x, t)$ , and test function  $\psi^*(x, t)$ , can be approximated by a parameterized density  $\hat{p}(x, \alpha(t))$  and test function  $\hat{\psi}(x, \alpha(t))$ , respectively, so that all of the time dependence is captured by the variables  $\alpha(t) = (\alpha_1(t), \ldots, \alpha_N(t))$ . For example, a standard method for choosing a parameterization is to pick an exponential family (43), or specifically a collection of quasiequilibrium distributions (25). In this case, one selects a finite number of linearly independent functions of the state  $\{\phi_i(x)\}_{i=1}^N$  to serve as observables describing the system. The parameterized densities  $\hat{p}(x, \alpha(t))$  are defined as (for time dependent "natural" parameters  $\alpha(t)$ )

$$\hat{p}(x, \alpha(t)) = \exp\left(\sum_{i=1}^{N} \alpha_i(t)\phi_i(x) + \mathcal{F}(\alpha(t))\right),$$

where  $\mathcal{F}(\alpha) = -\log \left(\int \exp\left(\sum_{i=1}^N \alpha_i \phi_i(x)\right) \mathrm{d}x\right)$  is a log-normalizing constant. The primary reason for using this parameterization is that for each  $\alpha$ , this  $\hat{p}(x,\alpha)$  has maximum Shannon entropy with respect to all other probability densities subject to the constraint that the averages  $\langle \phi_i(x) \rangle_{\hat{p}}$  take on prescribed values. In the quasiequilibrium case,  $\phi_1(x)$  is almost always taken as the system energy, and hence  $\alpha_1(t)$  becomes  $-\beta$ .

Given any parameterization, quasiequilibrium or otherwise, the dynamical equations (Eqs. 4 and 5) reduce to a coupled system of ordinary differential equations

$$\sum_{i=1}^{N} \{a_i, a_j\} \frac{\mathrm{d}a_j}{\mathrm{d}t} = \frac{\partial \mathcal{H}}{\partial a_i},\tag{6}$$

where

$$\{\alpha_i, \alpha_j\} = \int_X \frac{\partial \hat{\psi}}{\partial \alpha_i} \frac{\partial \hat{p}}{\partial \alpha_j} - \frac{\partial \hat{\psi}}{\partial \alpha_j} \frac{\partial \hat{p}}{\partial \alpha_i} dx.$$

The solution to Eq. 6,  $\alpha^*(t)$ , offers the best approximations to the true solution  $p^*(x, t) \approx \hat{p}(x, \alpha^*(t))$ ,  $\psi^*(x, t) \approx \hat{\psi}(x, \alpha^*(t))$ , lying within the parameterized subspace.

# Stochastic thermodynamics with internal variables

Finally, we fuse stochastic thermodynamics with this variational framework to provide a general method for constructing TIV

models. Stochastic thermodynamics provides the appropriate thermodynamic definitions, while the variational formalism of Eyink will allow us to derive dynamical equations for the internal variables consistent with the microscopic physics.

We return to the colloidal particle system with governing stochastic differential equation

$$dx(t) = -\frac{1}{\eta} \frac{\partial e}{\partial x}(x, \lambda) dt + \sqrt{2d} db(t)$$

If  $p(x, t \mid \lambda)$  is the probability density of observing the system in state x at time t given a prespecified external protocol,  $\lambda(t)$ , then  $p(x, t \mid \lambda)$  obeys the Fokker–Planck equation

$$\frac{\partial p}{\partial t} = \mathcal{L} \ p = \frac{1}{\eta} \frac{\partial}{\partial x} \cdot \left( \frac{\partial e}{\partial x} \ p \right) + d\Delta_x p.$$

When  $\lambda(t)$  is held constant, the true density tends toward the equilibrium Boltzmann distribution,  $p^*(x, t \mid \lambda) \propto \exp(-\beta e(x, \lambda))$ . Away from equilibrium,  $p^*(x, t | \lambda)$  may be highly complex, and in that case, we would like to find a low-dimensional representation which captures the physical phenomena of interest. To do so, we choose a class of parameterized densities  $\hat{p}(x, a)$  to use in the variational method of Eyink, keeping in mind that the variables  $\alpha(t)$  are to become the internal variables in the macroscopic description. This is in direct analogy with the assumption of a uniform probability density in the microcanonical ensemble, or the Maxwellian distribution in the canonical ensemble. Note that since displacement (or strain) is controlled rather than force (or stress), we assume no explicit dependence on the external protocol  $\lambda$  in  $\hat{p}(x, \alpha)$ . This will prove necessary mathematically in what follows. Finally, we do not explicitly consider the dependence of  $\hat{p}$  on  $\beta$ , as we have assumed that temperature is constant.

We next define the approximate entropy  $\hat{s}(x, \alpha) = -k_B \log (\hat{p}(x, \alpha))$  and use its derivatives with respect to the internal variables to define the test function in the variational formalism

$$\hat{\psi}(x, \alpha, \gamma) = 1 + \gamma \cdot \frac{\partial \hat{s}}{\partial \alpha}$$

Since the true solution to the adjoint equation  $\frac{\partial \psi^*}{\partial t} = -\mathcal{L}^\dagger \psi^*$  is  $\psi^* \equiv \text{const.}$ , the variables  $\gamma$  serve as expansion coefficients about the true solution  $\psi^* \equiv 1$ . In SI Appendix, we show that they essentially function as dummy variables, as the variational solution fixes  $\gamma(t) \equiv 0$  for all time. Hence, the vector  $\alpha(t)$  will be the only relevant variable. Assuming this choice of density and test function, the variational formalism of Eyink yields the dynamical equation

$$\left\langle \frac{\partial \hat{\mathbf{S}}}{\partial \alpha} \frac{\partial \hat{\mathbf{S}}^{\mathrm{T}}}{\partial \alpha} \right\rangle_{\hat{p}} \cdot \dot{\alpha} = -k_{\mathrm{B}} \left\langle \mathcal{L}^{\dagger} \frac{\partial \hat{\mathbf{S}}}{\partial \alpha} \right\rangle_{\hat{p}},\tag{7}$$

where  $\langle g \rangle_{\hat{p}} = \int g(x) \hat{p}(x, a) dx$  denotes averaging with respect to  $\hat{p}$ . This equation reveals the utility of our choice of  $\hat{\psi}$ . The matrix on the left-hand side  $\mathbb{F}_{ij} = \langle \frac{\partial \hat{E}}{\partial \alpha_i} \frac{\partial \hat{E}}{\partial \alpha_j} \rangle_{\hat{p}}$  is  $k_B^2$  times the Fisher information matrix of the density  $\hat{p}(x, a)$  (25). This matrix is always symmetric and is positive definite so long as the functions  $\{\frac{\partial \hat{E}}{\partial \alpha_i}(x, a)\}_{i=1}^N$  are linearly independent as functions of x for all  $\alpha$ . Picking  $\alpha(0)$  such that  $\hat{p}(x, \alpha(0)) \approx p^*(x, 0 \mid \lambda)$ , and using Eq. 7 to solve for  $\alpha(t)$  gives us the variational solution for  $\hat{p}(x, \alpha(t)) \approx p^*(x, t \mid \lambda)$  for all time.

Having approximated the density using the internal variables, we turn to stochastic thermodynamics to impose the thermodynamic structure. In order to make use of the approximate density,  $\hat{p}$ , we simply use the stochastic thermodynamics definitions of thermodynamic quantities at the macroscale, but make the

substitution  $p^*(x, t | \lambda) \rightarrow \hat{p}(x, \alpha(t))$ . Following this rule, we generate the thermodynamic quantities as

$$\hat{E}(\alpha, \lambda) = \langle e \rangle_{\hat{P}}$$

$$\hat{S}(\alpha) = -k_{B} \langle \log (\hat{P}) \rangle_{\hat{P}}$$

$$\hat{A}^{\text{neq}}(\alpha, \lambda) = \hat{E} - T\hat{S}$$

$$\frac{d}{dt} \hat{W}(\alpha, \lambda) = \langle \frac{\partial e}{\partial \lambda} \hat{\lambda} \rangle_{\hat{P}}$$
(8)

$$T\frac{d}{dt}\hat{S}tot(\alpha,\lambda) = \frac{d}{dt}\hat{W} - \frac{d}{dt}\hat{A}^{neq}$$
 (9)

$$\frac{\mathrm{d}}{\mathrm{d}t}\hat{S}m(\alpha,\lambda) = \frac{\mathrm{d}}{\mathrm{d}t}\hat{S}\cot - \frac{\mathrm{d}}{\mathrm{d}t}\hat{S},\tag{10}$$

where Eqs. 8-10 are derived from Eqs. 1 and 2, respectively, as shown in SI Appendix. Since we have assumed a constant bath temperature for the governing Langevin equation, we do not explicitly write the dependence of the quantities above on  $\beta$ . Recall, a key assumption is that the approximate density should be independent of  $\lambda$  for fixed  $\alpha$ . Hence, the approximate entropy,  $\hat{S}$ , is a function of  $\alpha$  alone. This means that the partial derivative with respect to  $\lambda$  can be factored out of the expectation in Eq. 8. Since  $\hat{S}$ does not depend on  $\lambda$ , we may write

$$\frac{\mathrm{d}}{\mathrm{d}t}\hat{W} = \frac{\partial \hat{E}}{\partial \lambda}\dot{\lambda} = \frac{\partial}{\partial \lambda}(\hat{E} - T\hat{S})\dot{\lambda} = \frac{\partial \hat{A}^{\mathrm{neq}}}{\partial \lambda}\dot{\lambda} \equiv \hat{F}ex\dot{\lambda},$$

so that the approximate external force is given by the gradient of  $\hat{A}^{\text{neq}}$  with respect to the external protocol,  $\hat{F}^{\text{ex}} \equiv \frac{\partial \hat{A}^{\text{neq}}}{\partial \lambda}$ . Moreover, Eqs. 9 and 10 simplify to

$$T\frac{d}{dt}\hat{S}tot = -\frac{\partial \hat{A}^{neq}}{\partial \alpha} \cdot \dot{\alpha} \quad \frac{d}{dt}\hat{Q} = -\frac{\partial \hat{E}}{\partial \alpha} \cdot \dot{\alpha}.$$

Thus, the approximate work rate and the approximate rate of entropy production of the medium are given by the derivatives of Ê and the approximate work rate and the approximate rate of total entropy production are given by the derivatives of Âneq. In particular, the rate of total entropy production takes the form of a product of fluxes,  $\dot{\alpha}$ , and affinities,  $\mathcal{A}_{\alpha}=-\frac{\partial\hat{A}^{\mathrm{neq}}}{\partial\alpha}$ . Likewise, the internal variables do not explicitly enter into the equation for the work rate, just as in TIV. Moreover, in SI Appendix, we prove that for an arbitrary interaction energy  $e(x, \lambda)$ , internal variables obey the stronger GENERIC structure (44), obeying a gradient flow equation with respect to the nonequilibrium free energy, whenever the approximate probability density is assumed to be Gaussian. In this case, the internal variables are the mean and inverse covariance  $(\alpha = (\mu, \Sigma^{-1}))$  of the probability density of the state,  $x \in \mathbb{R}^N$ . Symbolically, we define

$$\hat{p}(\mathbf{x}, \boldsymbol{\mu}, \boldsymbol{\Sigma}^{-1}) = \sqrt{\det\left(\frac{\boldsymbol{\Sigma}^{-1}}{2\pi}\right)} \exp\left(-\frac{1}{2}(\mathbf{x} - \boldsymbol{\mu})^{\mathrm{T}} \boldsymbol{\Sigma}^{-1}(\mathbf{x} - \boldsymbol{\mu})\right). \tag{11}$$

This choice of form for the approximate density is a standard choice in popular approximation methods including Gaussian phase packets (45, 46) and diffusive molecular dynamics (47, 48) primarily for its tractable nature.

As mentioned, the dynamics of  $\mu$  and  $\Sigma^{-1}$  are given in terms of gradients with respect to the nonequilibrium free energy

$$\dot{\mu} = -\frac{1}{\eta} \frac{\partial \hat{A}^{\text{neq}}}{\partial u}, \quad \dot{\Sigma}^{-1} = -M(\Sigma^{-1}): \frac{\partial \hat{A}^{\text{neq}}}{\partial \Sigma^{-1}}$$
 (12)

for a positive semidefinite dissipation tensor  $M(\Sigma^{-1})$ , and hence, the total rate of entropy production is guaranteed to be nonnegative

$$T\frac{\mathrm{d}}{\mathrm{d}t}\hat{S}^{\mathrm{tot}} = \frac{1}{\eta} \left\| \frac{\partial \hat{A}neq}{\partial \mu} \right\|^{2} + \frac{\partial \hat{A}neq}{\partial \Sigma^{-1}} : M: \frac{\partial \hat{A}neq}{\partial \Sigma^{-1}}.$$
 (13)

Thus, we see that the thermodynamic structure emerges naturally by utilizing the variational method of Eyink within the context of stochastic thermodynamics, and that we are not forced to postulate phenomenological equations for  $\alpha(t)$ . They emerge directly from the variational structure.

To illustrate the STIV framework, we apply it to a toy model: an

#### Results

#### A single colloidal particle

overdamped, colloidal particle acted on by an external force that is linear in the extension of a spring connected to the particle. Despite its simplicity, this model is often used to describe a molecule caught in an optical trap. In one dimension, the governing Langevin equation for the particle's position is given by  $dx = -\frac{1}{n} \frac{\partial e}{\partial x}(x, \lambda) dt + \sqrt{2d} db$ , where  $e(x, \lambda) = \frac{k}{2}(\lambda - x)^2$  is the energy of the spring or the trapping potential, and  $\lambda(t)$  is an arbitrary external protocol. The corresponding Fokker-Planck operator is  $\mathcal{L} p = \frac{1}{n} \frac{\partial}{\partial x} (\frac{\partial e}{\partial x} p) + d \frac{\partial^2}{\partial x^2} p$ . The true solution is an Ornstein-Uhlenbeck (OU) process, thus, providing an exactly solvable model for comparison (49). Since the probability density of the OU process is Gaussian for all time (assuming a Gaussian initial distribution), we use a Gaussian approximate distribution with mean  $\mu$  and standard deviation  $\sigma$  as internal variables (Eq. 11 with  $\Sigma^{-1} = 1/\sigma^2$ ). It is straightforward to input this density into the variational formalism of Eyink and compute the dynamics. The details of the derivation are written out in SI Appendix. The resulting dynamical equations recover the analytical solution for the OU process

$$\dot{\mu} = -\frac{k}{\eta}(\mu - \lambda), \quad \dot{\sigma} = -\frac{k}{\eta}\sigma\left(1 - \frac{1}{k\beta\sigma^2}\right).$$

Analysis of the phase diagram for these equations reveals that  $\mu$  exponentially relaxes toward the external protocol  $\lambda$ , and  $\sigma$  tends to  $\frac{1}{\sqrt{k\beta}}$  whenever  $\sigma(t=0) > 0$ .

Now that we have the dynamics, we turn to computing the thermodynamics quantities. Of particular interest is the fact that the fluxes of the internal variables are linear in the affinities,  $-\frac{\partial \hat{A}^{\text{neq}}}{\partial u} = \eta \dot{\mu}, -\frac{\partial \hat{A}^{\text{neq}}}{\partial \sigma} = \eta \dot{\sigma}$ , hence ensuring a nonnegative entropy production. We can also find the approximate work rate, heat rate, and rate of total entropy production explicitly

$$\frac{\mathrm{d}}{\mathrm{d}t}\hat{W} = \eta\dot{\mu}\dot{\lambda}, \quad \frac{\mathrm{d}}{\mathrm{d}t}\hat{Q} = \eta\dot{\mu}^2 - k\sigma\dot{\sigma}, \quad T\frac{\mathrm{d}}{\mathrm{d}t}\hat{S}^{\mathrm{tot}} = \eta\dot{\mu}^2 + \eta\dot{\sigma}^2.$$

Although a toy system, this example highlights the fact that when the true solution to the governing partial differential equation (PDE) for the probability density lies in the subspace spanned by the trial density, the true solution is recovered and relevant thermodynamic quantities can be exactly computed via the nonequilibrium free energy, as can be seen in Fig. 2.

# Double-well colloidal mass-spring-chain

For our primary example, we study a colloidal mass-spring-chain system with double-well interaction between masses. Depicted in

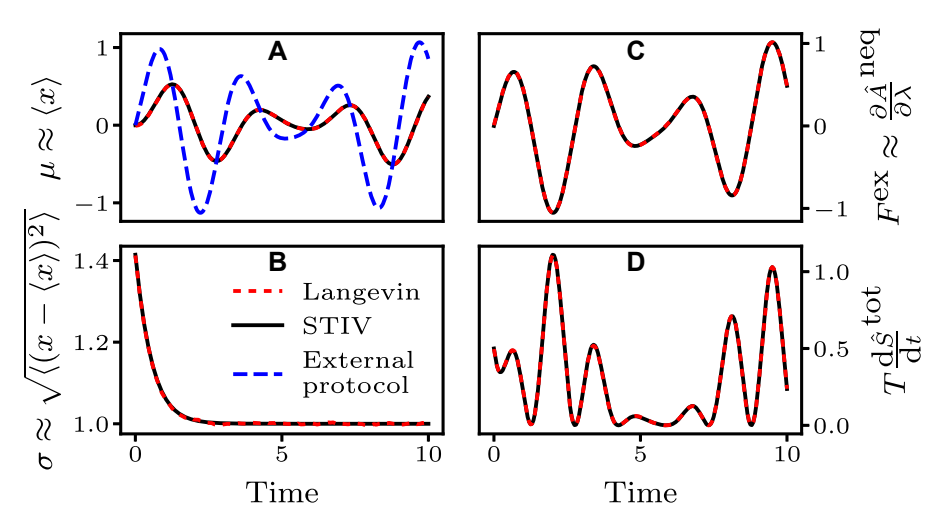


**Fig. 2.** A comparison of the STIV method (black solid line) to Langevin simulations (red short dashes, 100,000 simulations) for a single colloidal particle in a harmonic optical trap. A) The mean mass position,  $\mu \approx \langle x \rangle$ , as well as the external pulling protocol,  $\lambda(t)$ , in blue long danshes. B) The standard deviation,  $\sigma \approx \sqrt{\langle (x - \langle x \rangle)^2 \rangle}$ , of mass positions. C) The external force on the optical trap. D) The total rate of entropy production.

the inset of Fig. 3E, this model of phase front propagation in coiled-coil proteins and double-stranded DNA contains several metastable configurations corresponding to the different springs occupying one of the two minima in the interaction energy, and exhibits phase transitions between them. A key test for the STIV framework is whether or not the phase can accurately be predicted, and more importantly, whether the kinetics and thermodynamics of phase transitions can be captured without phenomenological kinetic equations. An almost identical model to the one studied here is considered in Truskinovsky and Vainchtein (50), but in a Hamiltonian setting rather than as a colloidal system. Here, the authors make use of the piecewise linearity of the force,  $-\frac{\partial e}{\partial x}$ , to derive an exact solution for the strain in the presence of a phase front traveling at constant velocity, and the kinetic relation for this phase front without the use of phenomenological assumptions. Our solution, on the other hand, is inherently approximate (though accurate), but does not depend on either the assumptions of constant velocity of the phase front, or the specific piecewise linear form of the force. The choice of interaction potential is simply convenience, and the STIV method could be easily applied to quartic or other double-well interaction potentials.

We assume each spring has internal energy described by the following double-well potential:

$$u(z) = \begin{cases} \frac{k_1}{2} (z + l_1)^2 & x \le 0\\ \frac{k_2}{2} (z - l_2)^2 + h_2 & x > 0, \end{cases}$$

where  $h_2$  is chosen so that u(z) is continuous (i.e.  $h_2=(k_1l_1^2-k_2l_2^2)/2$ ). For simplicity, we have placed one well on each side of the origin so that the transition point falls at z=0. Letting  $\mathbf{x}=(x_1,\ldots,x_N)$  be the positions of the N interior masses, the total energy, given an external protocol  $\lambda$ , is  $e(\mathbf{x},\lambda)=\sum_{i=1}^N u(x_i-x_{i-1})+u(\lambda-x_N)$ , where  $x_0\equiv 0$ .

We begin by assuming that the positions of the masses can be well described using a multivariate Gaussian distribution, and set the internal variables to be the mean  $\mu$  and the inverse covariance  $\Sigma^{-1}$  as in Eq. 11. The exact form of the dynamical equations for the

internal variables induced by the STIV framework can be found in the SI Appendix. As expected, the equations obey the gradient flow structure given by Eq. 12, where in this case, we have  $M_{ij,kl} = \frac{1}{\eta} (\Sigma_{ik}^{-1} \Sigma_{jl}^{-2} + \Sigma_{ik}^{-2} \Sigma_{jl}^{-1} + \Sigma_{il}^{-1} \Sigma_{jk}^{-2} + \Sigma_{il}^{-2} \Sigma_{jk}^{-1}). \text{ The rate of total entropy production, given by Eq. 13, is thus nonnegative. It is interesting to note that the dynamical equations for <math display="inline">\mu$  and  $\Sigma^{-1}$  are coupled through an approximation of the phase fraction of springs occupying the right well

$$\hat{\Phi}_{i}(x, t) \equiv \int_{-\infty}^{\infty} \mathbb{1}_{(x_{i}-x_{i-1}>0)} \hat{p}(x, \mu(t), \Sigma^{-1}(t)) dx.$$

As an important special case, fixing the interaction parameters to produce a quadratic interaction,  $l_1=-l_2$  and  $k_1=k_2=k$ , causes the dependence on  $\hat{\Phi}$  to drop out, and the equations from  $\mu$  and  $\Sigma^{-1}$  decouple.

In Fig. 4, we show a comparison of the probability densities produced by the STIV framework for a two mass system to those obtained from Langevin simulations of the governing stochastic differential equation. Although fine details of the multimodal structure are missed (as is to be expected when using a Gaussian model), the size and location of the dominant region of nonzero probability is captured, making it possible to compute the relevant macroscopic thermodynamic quantities, as we discuss next.

Since the STIV framework requires an approximation to the true density of states using internal variables, we verify the accuracy of the Gaussian model for the double-well mass-springchain system using macroscopic thermodynamic quantities including the phase fraction, external force, and total rate of entropy production. As the exact form of the true solution  $p^*(x, t \mid \lambda)$  is unknown, we compare the results to Langevin simulations of a system with eight free masses in Fig. 3. Despite the fact that the true solution is multimodal due to the existence of several metastable configurations, it is clear that the approximations of the mean mass position (A), phase fraction (B), external force  $(\frac{\partial E}{\partial \lambda} \approx \frac{\partial \hat{E}}{\partial \lambda} = \frac{\partial \hat{A}^{\text{neq}}}{\partial \lambda})$  (C), and total rate of entropy production (D) are all highly accurate. This holds true for a variety of pulling protocols including linear (1), sinusoidal (2), and a step displacement (3, 4), as well as for symmetric (1, 2, 3) and asymmetric (4) interaction potentials. Returning to (B), we see that for a system

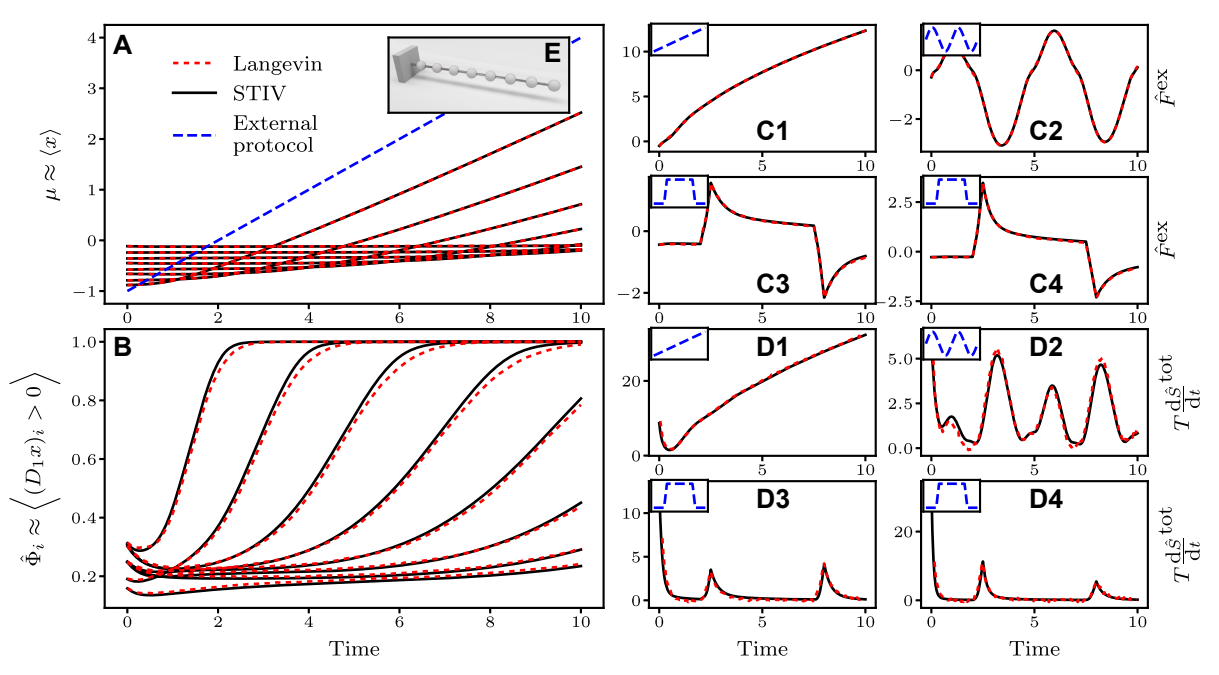


Fig. 3. A) A comparison of the predicted mean mass locations using STIV (black solid lines) and empirical mean of 100,000 Langevin simulations (red short dashes) for the 8 mass colloidal mass-spring-chain with double-well interactions and a linear external protocol (external protocol shown in blue long dahses throughout). Except in C4) and D4), the parameters of the symmetric interaction potential are  $k_1 = k_2 = l_1 = l_2 = 1$ . B) The predicted and simulated phase fractions of springs in the right well for the same system as A). C) The predicted vs. simulated external force for four different pulling protocols: (1) linear, (2) sinusoidal, (3) step, (4) step with an asymmetric interaction potential between masses  $(k_1 = 1, l_1 = 1, k_2 = 2, l_2 = 1/2)$ . D) The predicted vs. simulated rate of total entropy production for the same four pulling protocols as in C). The external protocols used are shown in the insets of C), D). E) Cartoon of the mass-spring-chain configuration. One side is held fixed, while the other is controlled by the external protocol.

with an initial configuration in which all the springs begin in the left well we can observe a propagating phase front as the springs, one by one, transition from the left to the right well. This transition is captured by the internal variable model with high accuracy allowing one to directly approximate the velocity of the phase front. We note, however, that the quantitative accuracy of the method appears to hold most strongly in the case that the thermal energy is significantly larger or smaller than the scale of the energy barrier separating the two potential energy wells in the spring interaction. When the thermal energy and potential energy barriers are at the same scale, the true density of states is highly multimodal, and not well approximated by a multivariate Gaussian, see Movie S1. In this case, the STIV approximation captures the behavior of only the dominant mode. When the thermal energy is large relative to the barrier, the thermal vibrations cause the modes to collapse into a single "basin" which can be well approximated by the STIV density, see Movie S2. Finally, when the thermal energy is small, the true density is unimodal, and undergoes rapid jumps between the different energy minima. In this regime, the Gaussian STIV density, again, becomes an effective choice for approximation.

The dynamical equations for the internal variables take the form of a discretized PDE. Assuming we properly rescale the parameters of the interaction potential, the viscosity, and temperature so that the equilibrium system length, energy, entropy, and quasistatic viscous dissipation are independent of the number of masses ( $l_i = l_i^0/N$ ,  $k_i = Nk_i^0$ ,  $\eta = \eta^0/N$ ,  $\beta = N\beta^0$  ( $i \in \{1, 2\}$ )) then, in the limit as the number of masses tends to infinity, the internal variables  $\mu_i$  and  $\Sigma_{ii}^{-1}$  become functions of continuous variables  $x \in$ [0, 1] and  $x, y \in [0, 1] \times [0, 1]$ , respectively. Since it is challenging to invert a continuum function  $\Sigma^{-1}(x, y, t)$ , we make use of the identity  $\dot{\Sigma}_{ij} = -(\Sigma \dot{\Sigma}^{-1} \Sigma)_{ij}$  to derive the following limiting PDE for  $\mu(x, t)$ ,  $\Sigma(x, y, t)$ , the strain,  $\epsilon(x, t) \equiv \frac{\partial \mu}{\partial x}(x, t)$ , and the covariance of the strain,  $\mathcal{E}(x, y, t) \equiv \frac{\partial^2 \Sigma}{\partial x \partial y}(x, y, t)$ 

$$\begin{split} &\frac{\partial \mu}{\partial t} = \frac{1}{\eta_0} \frac{\partial}{\partial x} \left\{ k_1^0 \left( \epsilon + l_1^0 \right) (1 - \hat{\Phi}) + k_2^0 \left( \epsilon - l_2^0 \right) \hat{\Phi} + (k_2^0 - k_1^0) \mathcal{E} \frac{\partial \hat{\Phi}}{\partial \epsilon} \right\} \\ &\frac{\partial \Sigma}{\partial t} = 2 \Delta^{\text{tt}} \Sigma \\ &\mu(x = 0, \, t) = 0, \quad \mu(x = l_0, \, t) = \lambda(t) \\ &\Sigma(x = 0, \, y, \, t) = \Sigma(x = l_0, \, y, \, t) = 0 \\ &\Sigma(x, \, y = 0, \, t) = \Sigma(x, \, y = l_0, \, t) = 0, \end{split}$$

with the approximate phase fraction defined through

$$\hat{\Phi}(x, t) = \hat{\Phi}(\epsilon, \mathcal{E}) = \Phi\left(\frac{\epsilon(x, t)}{\sqrt{\mathcal{E}(x, x, t)}}\right).$$

Here, 
$$\Delta^w = \frac{\partial}{\partial x} w(x,t) \frac{\partial}{\partial x} + \frac{\partial}{\partial y} w(y,t) \frac{\partial}{\partial y}, \quad w(x,t) = \frac{k_1^0}{\eta^0} (1-\hat{\Phi}) + \frac{k_2^0}{\eta^0} \hat{\Phi} - \frac{1}{\eta^0} (k_1^0 l_1^0 + k_2^0 l_2^0) \frac{\partial \hat{\Phi}}{\partial \epsilon},$$
 and  $\Phi(\xi)$  is the cumulative distribution function of a standard Gaussian (mean zero, variance one). Both equations for  $\frac{\partial u}{\partial t}$  and  $\frac{\partial v}{\partial t}$  contain contributions from the left well (the terms multiplying  $(1-\hat{\Phi})$ ), the right well (the terms multiplying  $\hat{\Phi}$ ), and the phase boundary (the terms multiplying  $\frac{\partial \hat{\Phi}}{\partial t}$ ), and in SI Appendix, we

phase boundary (the terms multiplying  $\frac{\partial \hat{\mathbf{0}}}{\partial c}$ ), and in SI Appendix, we give assumptions on the continuum limit for  $\Sigma(x, y, t)$  such that these dynamical equation maintain the gradient flow structure

$$\begin{split} \frac{\partial \mu}{\partial t} &= -\frac{1}{\eta} \frac{\delta \hat{A} n e q}{\delta \mu} \\ \frac{\partial \sigma}{\partial t} &= -\int_0^1 \! \int_0^1 M(x,\,y,\,z,\,w,\,t) \frac{\delta \hat{A} n e q}{\delta \Sigma}(z,\,w,\,t) dz dw. \end{split}$$

In Fig. 5A, we demonstrate that the continuum response of the system can be well approximated through the STIV framework with

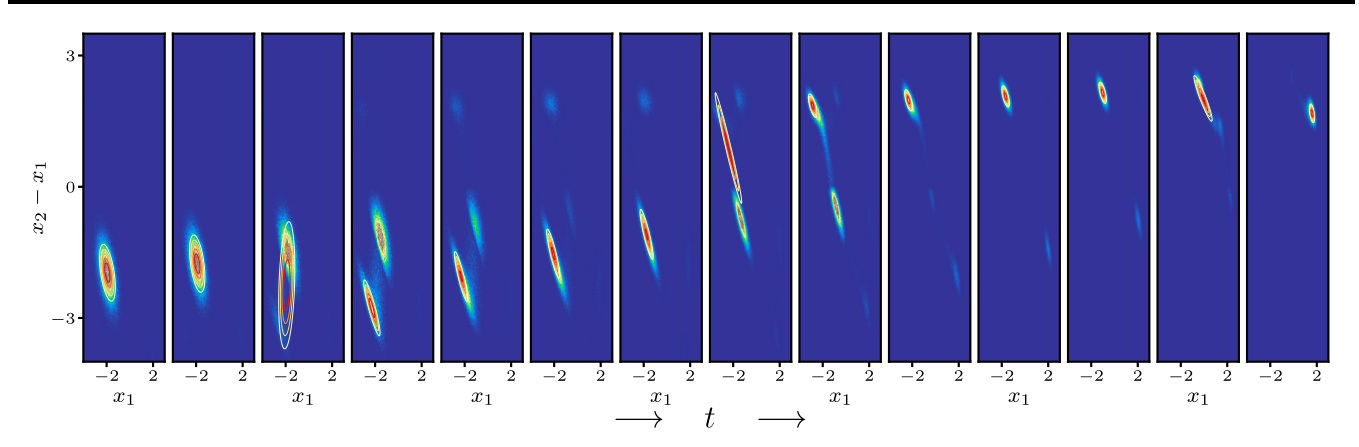


Fig. 4. A comparison of the probability density for the spring lengths for a two mass mass–spring–chain system with double-well spring energies. The colored histograms depict densities collected from 100,000 Langevin simulations of the solution to the governing stochastic differential equation, while the colored contour lines show the approximation using STIV. On each panel, the horizontal axis gives the length of the first spring,  $x_1$ , and the vertical axis gives the length of second,  $x_2 - x_1$ . Panels from left to right show equal increments in time. We see that despite missing the details of the multimodal behavior apparent in the Langevin simulations, the STIV approximation successfully tracks the location and size of the dominant region of nonzero probability.

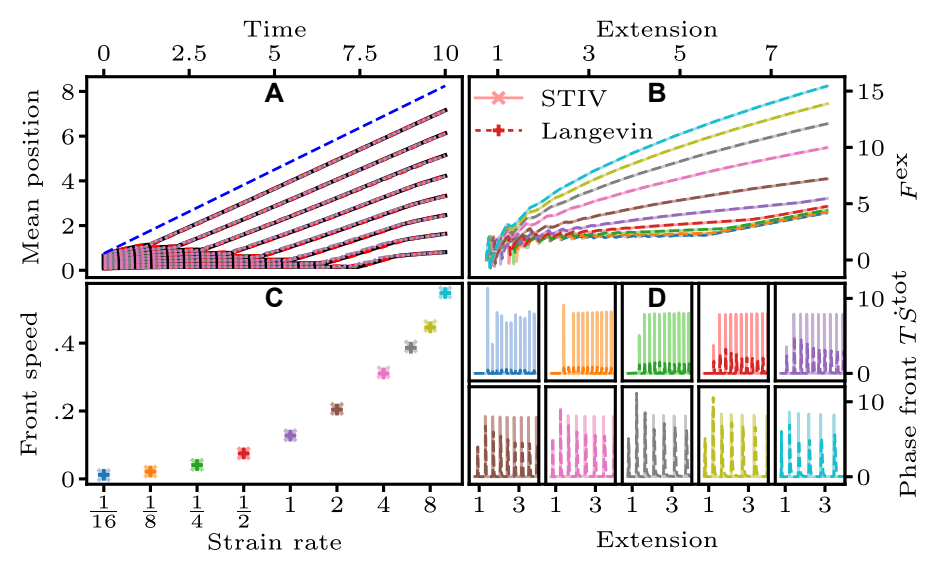


Fig. 5. A) Mean mass positions for Langevin and STIV approximations to a 17 mass (Langevin: red short dashes, STIV: solid black) and a 62 mass (Langevin: pink short dashes, STIV: gray long dashes) double-well mass-spring-chain system, with parameters rescaled for the same effective behavior. For both systems, only the eight masses expected to overlap are plotted. Throughout (B, C, D), darker colors, dashed lines, and + scatter points denote results from Langevin simulations, whereas lighter colors, solid lines, and × scatter points denote results from the STIV approximation. B) The external force as a function of extension for the 17 mass system at 10 different strain rates (shown in C). C) The phase front speed as a function of strain rate in the 17 mass system. D) The rate of entropy production due to the phase front as a function of extension for each of the strain rates shown in C).

finitely many masses. We see agreement between the mean mass positions observed in Langevin simulations and those predicted using the STIV framework for both 17 and 62 masses, verifying that both discretizations capture the continuum response. This allows us to use the 17 mass system to accurately predict important continuum level quantities such as the external force as a function of extension,  $\lambda$ , Fig. 5B, the phase front speed, Fig. 5C, for different applied strain rates, and finally, the rate of entropy production due to the phase front, Fig. 5D, as a function of the system extension for each of the strain rates shown in (C). Methods for computing the front speed and the rate of entropy production due to the phase front can be found in SI Appendix.

Finally, in the continuum limit, one can differentiate in time the defining equation for the location of the phase front in the reference configuration,  $\hat{\Phi}(\hat{l}(t),t) \equiv \frac{1}{2}$  to yield the following ordinary differential equation for the location of the phase front

$$\frac{d}{dt}\hat{I}(t) = -\frac{\frac{\partial^2}{\partial x^2}\frac{\partial\hat{A}^{\rm neq}}{\partial \varepsilon}(x,\,t)}{\eta\frac{\partial^2\mu}{\partial x^2}(x,\,t)}\Bigg|_{x=\hat{I}(t)}.$$

This equation reveals that the phase front velocity is directly proportional to the ratio of the curvature of the thermodynamic affinity conjugate to the strain  $\mathcal{A}_{\epsilon} \equiv -\frac{\delta\hat{A}^{\text{neq}}}{\delta\epsilon}$  and the curvature of  $\mu$  at the location of the phase front.

#### Discussion

Our results demonstrate the utility and accuracy of the STIV framework as a method for constructing TIV models which are consistent with microscopic physics. After assuming a functional form for a set of parameterized probability densities which serve to approximate the true density of states, inserting this approximation into the thermodynamic definitions taken from stochastic thermodynamics directly yields the internal variables structure, and the dynamics of these internal variables are fully determined by the variational method of Evink. The resulting macroscopic model encodes the microscopic features of the system to the degree allowed within the provided probability density without any need for further reference back to smaller scales. Moreover, in the important case of a Gaussian form for the approximate probability density,  $\hat{p}(x, \alpha)$ , we recover the gradient flow dynamics and the GENERIC structure which is commonly assumed without direct microscopic justification. In this work, we have focused on examples yielding analytically tractable approximations. However, it is equally possible to extend the method beyond such constraints by creating a numerical implementation based on sampling techniques using modern statistical and machinelearning techniques. Furthermore, extensions to Hamiltonian systems, active noise, and models exhibiting significant coarse graining constitute important future steps for the STIV framework.

# **Supplementary Material**

Supplementary material is available at PNAS Nexus online.

# **Funding**

T.L. acknowledges that this project was supported in part by a fellowship award under contract FA9550-21-F-0003 through the National Defense Science and Engineering Grauate Fellowship Program, sponsored by the Air Force Research Laboratory, the Office of Naval Research, and the Army Research Office. P.K.P. acknowledges support from ACS, USA (grant number PRF-61793 ND10). C.R. gratefully acknowledges support from NSF CAREER Award (CMMI-2047506).

#### **Author Contributions**

P.K.P. and C.R. designed the research. T.L. and C.R. carried out the research. T.L., P.K.P., and C.R. analyzed the results. T.L., P.K.P., and C.R. wrote the paper.

# **Preprints**

This document was posted on a preprint: https://arxiv.org/pdf/ 2309.07112.pdf

# **Data Availability**

Reproduction data for Figs. 2–5 can be found in Leadbetter et al. (51). Source code used to produce, analyze, and create figures from the data can be found in the github repository https:// github.com/tleadbe1/STIV.

#### References

1 Jaeger HM, Liu AJ. 2010. Far-from-equilibrium physics: an overview, arXiv, arXiv:1009.4874, preprint: not peer reviewed.

- 2 Army Research Lab. Complex dynamics and systems. ARL Broad Agency Announcement; 2020. [accessed 2023 Dec 12] https:// cftste.experience.crmforce.mil/arlext/s/baadatabaseentry/ a3Ft0000002Y394EAC/opt0018.
- Hemminger J, Fleming G, Ratner M. 2007. Directing matter and energy: five challenges for science and the imagination. Washington, DC: DOESC (USDOE Office of Science (SC)). Technical report.
- Connolly JAD. 2009. The geodynamic equation of state: what and how. Geochem Geophys Geosyst. 10(10):1-19.
- Gompper G, et al. 2020. The 2020 motile active matter roadmap. J Phys Condens Matter. 32(19):193001.
- Lebon G, Jou D, Casas-Vázquez J. 2008. Understanding nonequilibrium thermodynamics. Vol. 295. Berlin: Springer.
- Jou D, Casas-Vázquez J, Lebon G. 1996. Extended irreversible thermodynamics. Berlin: Springer.
- Maugin GA, Muschik W. 1994. Thermodynamics with internal variables. Part I. General concepts. J Non-Equil Thermody. 19: 217-249.
- Maugin GA, Muschik W. 1994. Thermodynamics with internal variables. Part II. Applications. J Non-Equil Thermody. 19:250–289.
- 10 Coleman BD. 1964. Thermodynamics of materials with memory. Arch Rat Mech Anal. 17(1):1-46.
- 11 Truesdell C. 1984. Historical introit: the origins of rational thermodynamics. In: Rational thermodynamics. Vol. 2. New York: Springer. p. 1-48. https://doi.org/10.1007/978-1-4612-5206-1.
- 12 Grmela M, Öttinger HC. 1997. Dynamics and thermodynamics of complex fluids. I. Development of a general formalism. Phys Rev E. 56(6):6620-6632.
- 13 Onsager L. 1931. Reciprocal relations in irreversible processes. I. Phys Rev. 37(4):405-426.
- 14 Doi M. 2011. Onsager's variational principle in soft matter. J Phys Condens Matter. 23(28):284118.
- 15 Mielke A. 2011. Formulation of thermoelastic dissipative material behavior using generic. Contin Mech Thermodyn. 23(3):233-256.
- 16 Jarzynski C. 1997. Nonequilibrium equality for free energy differences. Phys Rev Lett. 78(14):2690-2693.
- 17 Crooks GE. 1999. Entropy production fluctuation theorem and the nonequilibrium work relation for free energy differences. Phys Rev E. 60(3):2721-2726.
- Seifert U. 2005. Entropy production along a stochastic trajectory and an integral fluctuation theorem. Phys Rev Lett. 95(4):040602.
- 19 Seifert U. 2012. Stochastic thermodynamics, fluctuation theorems and molecular machines. Rep Prog Phys. 75(12):126001.
- 20 Horowitz JM, Gingrich TR. 2020. Thermodynamic uncertainty relations constrain non-equilibrium fluctuations. Nat Phys. 16(1): 15-20.
- 21 Feng J, Kurtz TG. 2006. Large deviations for stochastic processes. Vol. 131. Providence: American Mathematical Society.
- 22 Peletier MA. 2014. Variational modelling: energies, gradient flows, and large deviations, arXiv, arXiv:1402.1990, preprint: not peer reviewed.
- 23 Mielke A, Renger DRM, Peletier MA. 2016. A generalization of onsager's reciprocity relations to gradient flows with nonlinear mobility. J Non-Equil Thermody. 41(2):141-149.
- 24 Öttinger HC. 1998. General projection operator formalism for the dynamics and thermodynamics of complex fluids. Phys Rev E. 57(2):1416-1420.
- 25 Turkington B. 2013. An optimization principle for deriving nonequilibrium statistical models of hamiltonian dynamics. J Stat Phys. 152(3):569-597.

- 26 Pavelka M, Klika V, Grmela M. 2020. Generalization of the dynamical lack-of-fit reduction from generic to generic. J Stat Phys. 181(1):19–52.
- 27 Li X, Dirr N, Embacher P, Zimmer J, Reina C. 2019. Harnessing fluctuations to discover dissipative evolution equations. J Mech Phys Solids. 131:240–251.
- 28 Montefusco A, Peletier MA, Öttinger HC. 2021. A framework of nonequilibrium statistical mechanics. II. Coarse-graining. J Non-Equil Thermody. 46(1):15–33.
- 29 Eyink GL. 1996. Action principle in nonequilibrium statistical dynamics. Phys Rev E. 54(4):3419–3435.
- 30 Kreplak L, Doucet J, Dumas P, Briki F. 2004. New aspects of the  $\alpha$ -helix to  $\beta$ -sheet transition in stretched hard  $\alpha$ -keratin fibers. Biophys J. 87(1):640–647.
- 31 Torres-Sánchez A, Vanegas JM, Purohit PK, Arroyo M. 2019. Combined molecular/continuum modeling reveals the role of friction during fast unfolding of coiled-coil proteins. *Soft Matter*. 15(24):4961–4975.
- 32 Gore J, et al. 2006. DNA overwinds when stretched. Nature. 442(7104):836–839.
- 33 van Mameren J, et al. 2009. Unraveling the structure of dna during overstretching by using multicolor, single-molecule fluorescence imaging. Proc Natl Acad Sci U S A. 106(43): 18231–18236.
- 34 Parrondo JMR, Van den Broeck C, Kawai R. 2009. Entropy production and the arrow of time. *New J Phys.* 11(7):073008.
- 35 Still S, Sivak DA, Bell AJ, Crooks GE. 2012. Thermodynamics of prediction. Phys Rev Lett. 109(12):120604.
- 36 Seifert U. 2008. Stochastic thermodynamics: principles and perspectives. Eur Phys J B. 64(3-4):423–431.
- 37 Ortiz M, Stainier L. 1999. The variational formulation of viscoplastic constitutive updates. Comput Methods Appl Mech Eng. 171(3-4):419-444.

- 38 Nemat-Nasser S. 2004. Plasticity: a treatise on finite deformation of heterogeneous inelastic materials. Cambridge: Cambridge University Press.
- 39 Simo JC, Hughes TJR. 2006. Computational inelasticity. Vol. 7. New York: Springer Science & Business Media.
- 40 Gurtin ME, Fried E, Anand L. 2010. The mechanics and thermodynamics of continua. New York: Cambridge University Press.
- 41 Dunatunga S, Kamrin K. 2015. Continuum modelling and simulation of granular flows through their many phases. *J Fluid Mech.* 779:483–513.
- 42 Horstemeyer MF, Bammann DJ. 2010. Historical review of internal state variable theory for inelasticity. Int J Plast. 26(9):1310–1334.
- 43 Casella G, Berger RL. 2001. Statistical inference. Vol. 2. Pacific Grove: Duxbury.
- 44 Öttinger HC. 2005. Beyond equilibrium thermodynamics. Hoboken: John Wiley & Sons.
- 45 Heller EJ. 1975. Time-dependent approach to semiclassical dynamics. *J Chem Phys.* 62(4):1544–1555.
- 46 Gupta P, Ortiz M, Kochmann DM. 2021. Nonequilibrium thermomechanics of gaussian phase packet crystals: application to the quasistatic quasicontinuum method. J Mech Phys Solids. 153:104495.
- 47 Kulkarni Y, Knap J, Ortiz M. 2008. A variational approach to coarse graining of equilibrium and non-equilibrium atomistic description at finite temperature. *J Mech Phys Solids*. 56(4):1417–1449.
- 48 Li J, et al. 2011. Diffusive molecular dynamics and its application to nanoindentation and sintering. Phys Rev B. 84(5):054103.
- 49 Steele JM. 2001. Stochastic calculus and financial applications. Vol. 1. New York: Springer.
- 50 Truskinovsky L, Vainchtein A. 2005. Kinetics of martensitic phase transitions: lattice model. SIAM J Appl Math. 66(2):533–553.
- 51 Leadbetter T, Purohit PK, Reina C. 2023. A statistical mechanics framework for constructing non-equilibrium thermodynamic models. Dryad. https://doi.org/10.5061/dryad.kwh70rzbd